

UNITED STATES DEPARTMENT OF THE INTERIOR
GEOLOGICAL SURVEY

Focal Mechanisms of Near-shore Earthquakes Between Santa Barbara
and Monterey, California

by J. P. Eaton¹

Open-File Report 84-477

This report is preliminary and has not been reviewed for conformity with U.S. Geological Survey standards and stratigraphic nomenclature.

1. USGS Menlo Park, California

1984

INTRODUCTION

Focal mechanisms based on first motion directions were determined for six of the largest earthquakes that occurred near the coast of California between Santa Barbara and Monterey from 1978 to 1984. For this study appropriate records from both the northern California and southern California telemetered networks were played back from magnetic tape and were read for P-wave onset times and first motion directions, S-wave onset times (when legible), and maximum wave amplitudes and associated periods. Hypocenter determinations were based primarily on P-wave onset times and were calculated by the program HYPO 71 (Lee and Lahr, 1975). The crustal model used for each event was adjusted in an iterative process wherein it was sought to minimize the root-mean-square of onset time residuals as well as to separate the fields of compressions and dilatations on the first motion plots to permit double couple focal mechanism solutions. Except for the Santa Barbara earthquake, which occurred in a region of very abrupt lateral variation in the thickness of the low speed sedimentary section, station time corrections were all set equal to zero in the determination of hypocenters. Magnitudes were computed (by HYPO 71) from maximum amplitudes and associated periods by reducing the recorded amplitudes to equivalent Wood-Anderson amplitudes, which were then used with Richter's zero-magnitude-earthquake amplitude versus distance relationship to determine the magnitudes.

RESULTS

Epicenters, focal depths, magnitudes, crustal models, and focal planes for each of the six earthquakes studied are summarized in table 1. For each event, plane I is the preferred fault plane and plane II is the preferred auxiliary plane. First motion plots and focal planes for the earthquakes are shown in figure 1. The results are summarized graphically in figure 2, which shows selected faults of coastal central California as well as the locations, stylized focal plane solutions, and the two alternate interpretations of each solution.

In examining the individual earthquakes we shall proceed from south to north, which also corresponds to the order of occurrence of the four quakes larger than M5.0.

Santa Barbara M5.9 780813

Although based on more data, our fault plane solution is very similar to that obtained by Lee and others (1978). Our hypocenter is 1.9 km farther north and 1.2 km shallower than theirs. This difference results from different methods of compensating for the effect on seismic traveltimes of the thick sediments of the Santa Barbara and Ventura basins. Lee and others applied station corrections that were based on average residuals of 17 well recorded aftershocks to minimize relative location errors between events of the aftershock sequence. We attempted to remove the effects of the thick sediments to obtain a more accurate location for the main shock by using station corrections based on Pn-delay differences across the network from the recent, well recorded Lake Isabella earthquake of Oct. 21, 1983.

From 25 low-gain seismographs in 9 stations at epicentral distances between 265 km and 402 km we find average and median magnitude values of 5.9, with a smallest value of 5.4 and a largest value of 6.3. The M5.9 value that we find is much larger than the M5.1 (Pasadena) reported by Lee and others. We attribute the difference to a strong azimuthal variation in radiated wave amplitudes coupled with the narrow range in azimuths to the low-gain stations in the central Coast Ranges.

For the fault plane we prefer plane I, which strikes N64° W and dips 32° NE. In this solution the upper plate is thrust southwestward over the lower plate. The ratio of strike slip (left lateral) to dip slip (thrust) displacement is about 0.6 to 1.0. If projected up-dip all the way to the surface, this fault would outcrop near the central axis of the Santa Barbara Channel and would be parallel to mapped faults on the Channel floor (Jennings, 1975).

Santa Maria M4.0 820923

This event was the largest of a swarm of earthquakes that occurred south of Santa Maria during the fall of 1982. Its fault plane solution is similar to that for the Santa Barbara quake to the southeast. We have tentatively chosen plane I as the fault plane. It strikes N54° W and dips 56° NE. This solution corresponds to movement on a high angle reverse fault with the upper plate thrust over the lower plate in a southwesterly direction. The ratio of strike slip (left lateral) to dip slip (high angle reverse) displacement is about 0.5 to 1.0. If projected all the way to the surface the fault plane would outcrop in Solomon Canyon (along US 101 15 to 20 km south of Santa Maria) along a zone of Quarternary faulting (Jennings, 1975).

If plane II is the fault plane the fault strikes N 12° W and dips 42° SW. The upper plate moves northeasterly over the lower plate with a ratio of strike slip (right lateral) to dip slip (thrust) displacement of about 0.7 to 1.0.

Point Sal M5.1 800529

The fault plane solution for the Point Sal earthquake is quite similar to those for the Santa Maria and Santa Barbara earthquakes. However, the B-axis (intersection of the fault plane and auxiliary plane) dips about 5° toward the southeast instead of 15° to 22° toward the northwest, as was the case for those quakes. If the fault corresponds to focal plane I, it strikes N 62° W and dips 34° NE. In this solution the upper plate is thrust over the lower plate in a southwesterly direction. The ratio of strike slip (right lateral) to dip slip (thrust) displacement is about 0.16 to 1.0. If the fault plane corresponds to focal plane II it strikes N 72° W and dips 57° SW. In this solution the upper plate is thrust over the lower plate in a northeasterly direction. The ratio of strike slip (left lateral) to dip slip (high angle reverse) displacement is 0.11 to 1.0. For either solution the strike slip component is much less pronounced than for the two quakes considered earlier.

There is little basis for choosing between the two possibilities. Both solutions indicate a fault that strikes diagonally across the mapped strands of the Hosgri fault (Jennings, 1975) near the epicenter.

San Simeon M5.4 830829

In the fault plane solution for the San Simeon earthquake the B-axis dips toward the southeast much more steeply than for the Point Sal earthquake. This change continues the progressive rotation of the pattern of the focal sphere, around a horizontal NE-SW axis, that was established between the Santa Barbara and Santa Maria earthquakes and the Point Sal earthquake. Local geology also provides stronger support for choosing the fault plane for the San Simeon quake than for the Point Sal and Santa Maria quakes.

If focal plane I represents the fault, it strikes N 39° W and dips 55° NE. In this solution the fault is a right-lateral, high-angle reverse fault, with the upper plate (NE) sliding past and overriding the lower plate (SW) in a south-southeasterly direction. The ratio of strike slip (right lateral) to dip slip (high angle reverse) displacement is about 1.2 to 1.0. If projected all the way to the surface, the fault would outcrop just offshore, parallel the shoreline, and in-line with the onshore faults with Quaternary movement that run between Ragged Point and Point San Simeon (Jennings, 1975).

The fault that would correspond to the second focal plane would be left-lateral, high-angle, reverse oblique, striking N 77° E and dipping 58° SE. This solution appears to be incompatible with mapped faults in the region.

Pinon Peak M3.9 830721

This event was the largest of a swarm of earthquakes at the same location during July 1983. It occurred about 10 km from the coast in a complexly faulted region with both NW- and W- striking pre-Quaternary faults. In comparison with the San Simeon quake fault plane solution, the pattern of compressions and dilatations has rotated further around a horizontal NE - SW axis: the B-axis has rotated just past vertically downward to 84° NW.

If the fault corresponds to focal plane I, it strikes N 49° W and has a dip of 90°. In this solution the displacement is nearly pure right lateral strike slip. The strike is in agreement with the overall trends of the Palo Colorado and Coast Ridge faults, with which this quake might be associated (Jennings, 1975). If the fault corresponds to focal plane II, it would be a left-lateral strike slip fault with a strike of N 41° E and a dip of 84° NW. Because of the complexity of faulting near the epicenter, this possibility cannot be ruled out, although it seems less likely than the other solution.

Point Sur M5.2 830123

This event is the main shock of a main shock-aftershock sequence which it initiated. It occurred about 2 km east of the shoreline between the northern ends of the Palo Colorado and Sur faults and in-line with the southern end of

the San Gregorio-Palo Colorado fault across Monterey Bay (Jennings, 1977). Like the Pinon Peak quake, it has a fault plane solution with the b-axis nearly vertically downward.

If the fault corresponds to focal plane I, it strikes N 30° W and dips 78° NE. The displacement is nearly pure right lateral strike slip. If extended northwestward along strike, this fault plane virtually coincides with the southern end of the San Gregorio-Palo Colorado fault. If the fault plane corresponds to the second focal plane, it would be a left lateral strike slip fault striking N 88° E and dipping 77° NE. This solution is not in agreement with mapped faults in the region.

DISCUSSION

The focal plane solutions of the earthquakes reported here show a steady change in character in accordance with the location of the earthquakes. If measured with respect to a southeasterly azimuth, the dip of the B-axis varies from -15° and -22°, for the Santa Barbara and Santa Maria quakes, respectively, to +5° for Point Sal, to +39° for San Simeon, to +96° for Pinon Peak; and the B-axis is near vertically downward for the Point Sur quake. For the choices of fault planes indicated above, the corresponding progression in style of faulting is from left lateral reverse oblique, through simple reverse, to right lateral reverse oblique, and finally to right lateral strike slip. The three southernmost earthquakes, which lie in the Transverse Ranges, resulted from predominantly reverse faulting. The San Simeon quake, the southernmost of the three northern quakes, results from oblique faulting with nearly equal reverse and right lateral components. The two northernmost quakes resulted from nearly pure right lateral strike slip faulting.

TABLE 1

Locations, focal plane solutions, and crustal models for seven near-shore central California earthquakes. Focal plane parameters are strike and dip. The P-axis and B-axis are the directions of maximum compressive stress and of the line of intersection of the two focal planes. Their parameters are the strike and dip (inclination below horizontal) of the axis. The distance weighting factors applied to stations in the hypocenter determinations were 1.0 for distances less than x_{near} , diminished linearly from 1.0 to 0.1 between x_{near} and x_{far} , and were 0.0 for distances larger than x_{far} . The number pairs representing layers in the crustal models are the velocity (in km/sec) and depth to the top of the layer (in km). The displacement components characterizing the two possible solutions, corresponding to the fault plane being focal plane I or focal plane II, are abbreviated as follows: LS = left slip, RS = right slip, Rev = reverse, and Thr = thrust.

Figure 1

Focal plane plots for six near-shore earthquakes in central California.

Focal planes I and II correspond to the preferred fault plane and auxiliary plane, respectively. P and T are the directions of maximum and minimum compressive stress, respectively. B is the B-axis, the line of intersection of the two focal planes. Open circles represent dilatational first arrivals; closed circles, compressional first arrivals; and x's, conflicting first arrivals.

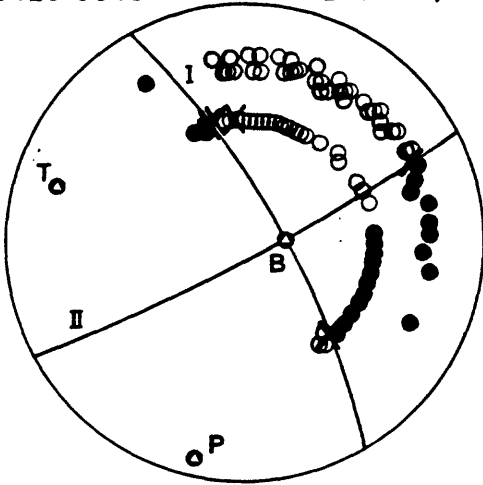
Summary data on the earthquakes and their focal plane solutions are presented in table 1.

Figure 2

Outline map of the coast of central California showing selected faults (from Jennings, 1975) and the locations, fault plane solutions, and alternate fault displacement diagrams for the earthquakes that were studied. In the fault displacement diagrams the strike and dip of the fault plane are indicated by the direction of the line segment and the appended numbers, respectively. For the oblique slip faults, the arrow indicates the direction of movement of the upper plate relative to the lower plate. The diagram for the preferred solution is on the left.

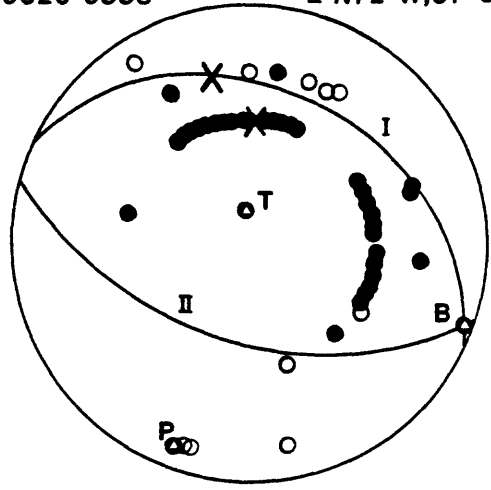
POINT SUR
840123 0540

I N30°W,78°NE
II N62°E,84°SE



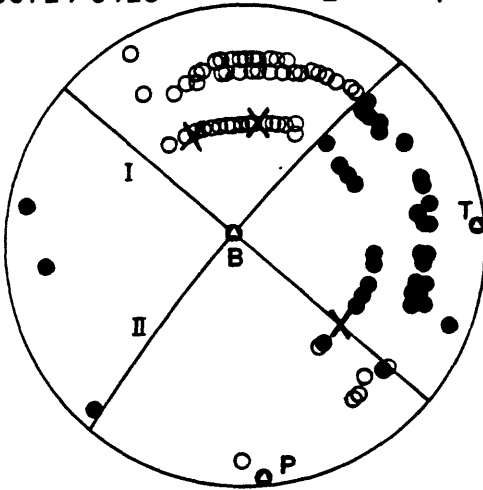
POINT SAL
800529 0338

I N62°W,34°NE
II N72°W,57°SW



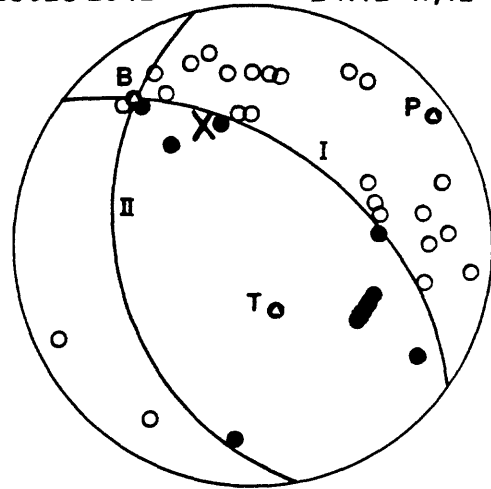
PINON PEAK
830721 0123

I N49°W,90°
II N41°E,84°NW



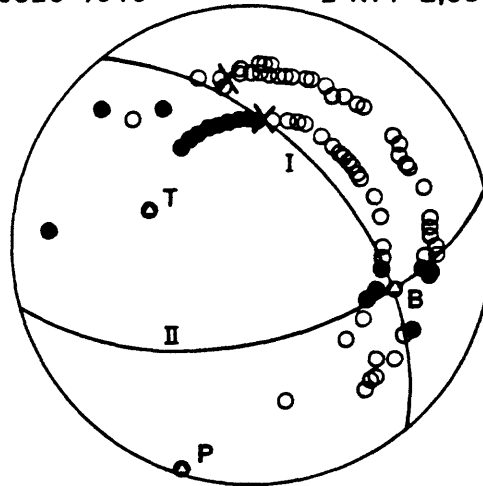
SANTA MARIA
820923 2042

I N54°W,56°NE
II N12°W,42°SW



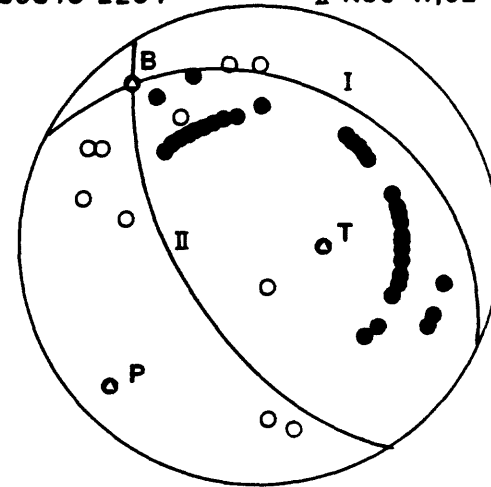
SAN SIMEON
830829 1010

I N39°W,55°NE
II N77°E,58°SE



SANTA BARBARA
780813 2254

I N64°W,32°NE
II N30°W,62°SW



REFERENCES

- Lee, W. H. K., Johnson, C. E., Henyey, T. L., and Yerkes, R. L., 1978, A Preliminary Study of the Santa Barbara, California, Earthquake of August 13, 1978 and its Major Aftershocks: U. S. Geological Survey Circular 797.
- Lee, W. H. K., and Lahr, J. C., 1975, HYP071(Revised): A computer program for determining hypocenter, magnitude, and first motion pattern of local earthquakes: U. S. Geological Survey Open-file Report 75-311, 114 p.
- Jennings, C. W., and others, 1975, Fault Map of California with Locations of Volcanoes, Thermal Springs and Thermal Wells: Map no. 1, - Faults, Volcanoes, Thermal Springs and Wells, California Geologic Data Map Series, California Division of Mines and Geology, State of California.

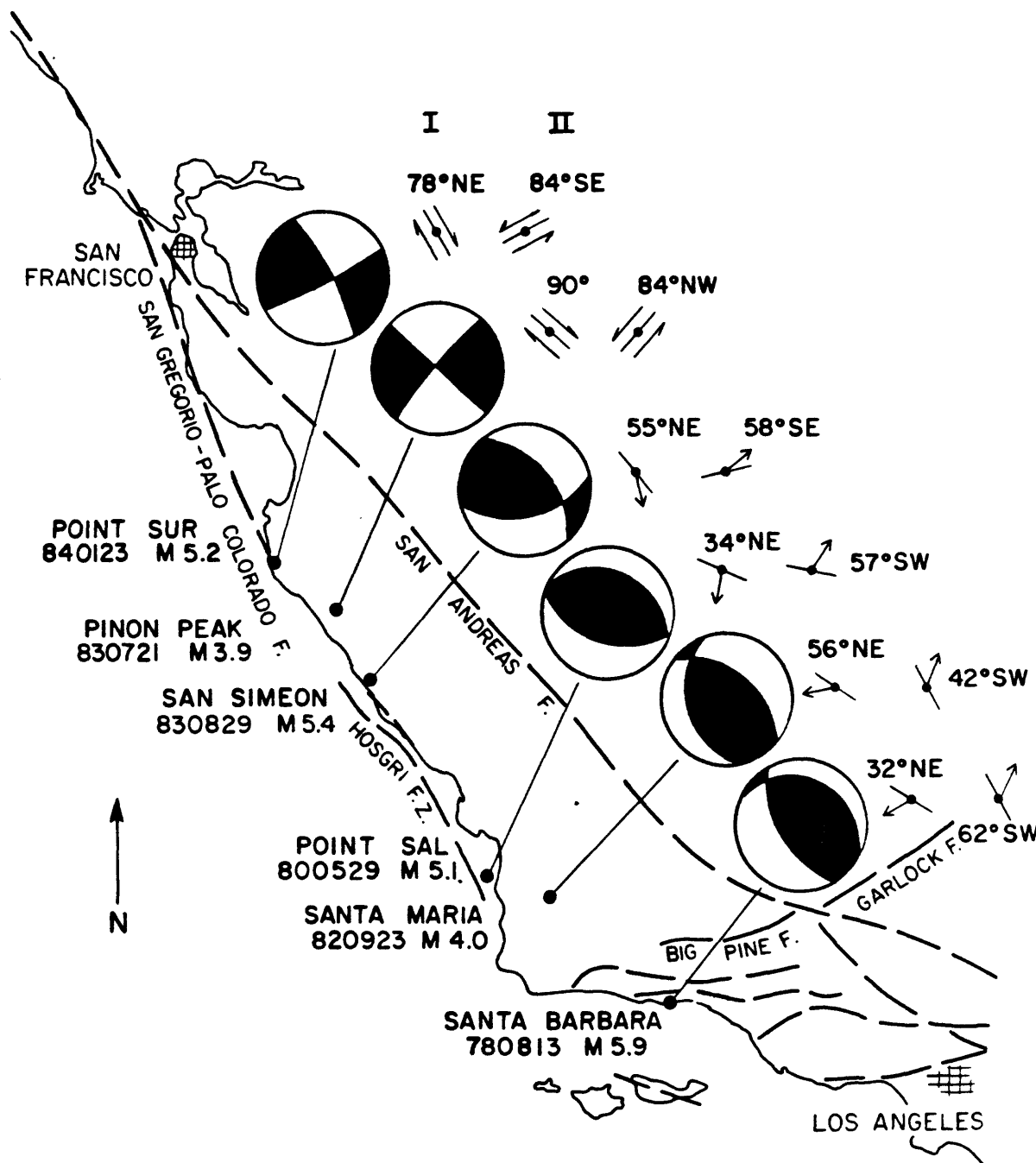


FIGURE 2

Table 1

Earthquake	Santa Barbara		Santa Maria		Point Sal		San Simeon		Pinon Peak		Point Sur	
	Date	Origin time	Date	Origin time	Date	Origin time						
	780813	2254 51.8	820923	2042 50.6	800529	0338 47.5	830829	1010 30.9	830721	0123 33.0	840123	0540 19.9
Latitude	32° 23.18'N	32° 23.18'N	34° 52.19'N	34° 52.19'N	34° 58.65'N	34° 58.65'N	35° 50.17'N	35° 50.17'N	36° 09.17'N	36° 09.17'N	36° 22.13'N	36° 22.13'N
Longitude	119° 42.60'W	119° 42.60'W	120° 21.76'W	120° 21.76'W	120° 42.37'W	120° 42.37'W	121° 20.70'W	121° 20.70'W	121° 32.64'W	121° 32.64'W	121° 52.74'W	121° 52.74'W
Depth	11.3 km	11.3 km	4.8 km	4.8 km	9.2 km	9.2 km	6.6 km	6.6 km	5.2 km	5.2 km	7.7 km	7.7 km
Magnitude	5.9	5.9	4.0	4.0	5.1	5.1	5.4	5.4	3.9	3.9	5.2	5.2
Focal Plane I	N64°W, 32°NE	N64°W, 32°NE	N54°W, 56°NE	N54°W, 56°NE	N62°W, 34°NE	N62°W, 34°NE	N39°W, 55°NE	N39°W, 55°NE	N49°W, 90°	N49°W, 90°	N30°W, 78°N	N30°W, 78°N
Focal Plane II	N30°W, 62°SW	N30°W, 62°SW	N12°W, 42°SW	N12°W, 42°SW	N72°W, 57°SW	N72°W, 57°SW	N77°E, 58°SE	N77°E, 58°SE	N41°E, 84°NW	N41°E, 84°NW	N62°E, 84°S	N62°E, 84°S
Paxis	S48°W, 15°SW	S48°W, 15°SW	N55°E, 8°NE	N55°E, 8°NE	S22°W, 11°SW	S22°W, 11°SW	S18°W, 2°SW	S18°W, 2°SW	S4°E, 4°SE	S4°E, 4°SE	S14°W, 9°SW	S14°W, 9°SW
Baxis	N38°W, 15°NW	N38°W, 15°NW	N39°W, 22°NW	N39°W, 22°NW	S69°E, 5°SE	S69°E, 5°SE	S73°E, 39°SE	S73°E, 39°SE	N49°W, 84°NW	N49°W, 84°NW	N88°E, 77°N	N88°E, 77°N
FP1 Displ.	0.57LS/1.0 Thr	0.57LS/1.0 Thr	0.50LS/1.0 Rev	0.50LS/1.0 Rev	0.15RS/1.0 Thr	0.15RS/1.0 Thr	1.18RS/1.0 Rev	1.18RS/1.0 Rev	RS	RS	RS	RS
FP2 Displ.	0.29RS/1/0 Rev	0.29RS/1/0 Rev	0.65RS/1.0 Thr	0.65RS/1.0 Thr	0.11LS/1.0 Rev	0.11LS/1.0 Rev	1.11LS/1.0 Rev	1.11LS/1.0 Rev	LS	LS	LS	LS
xnear	50 km	50 km	50 km	50 km	75 km	75 km	50 km	50 km	75 km	75 km	75 km	75 km
xfar	80 km	80 km	100 km	100 km	83 km	83 km	100 km	100 km	100 km	100 km	100 km	100 km
Model	2.50 0.0	2.50 0.0	3.00 0.0	3.00 0.0	3.00 0.0	3.00 0.0	3.00 0.0	3.00 0.0	3.00 0.0	3.00 0.0	3.00 0.0	3.00 0.0
"	4.50 2.0	4.50 2.0	5.70 1.5	5.70 1.5	5.60 1.5	5.60 1.5	5.70 1.5	5.70 1.5	5.70 1.5	5.70 1.5	5.70 1.5	5.70 1.5
"	5.50 6.0	5.50 6.0	6.00 6.0	6.00 6.0	6.30 13.0	6.30 13.0	6.30 8.0	6.30 8.0	6.20 8.0	6.20 8.0	6.20 8.0	6.20 8.0
"	6.10 10.0	6.10 10.0	6.40 12.0	6.40 12.0	8.00 26.0	8.00 26.0	6.50 13.0	6.50 13.0	6.40 12.0	6.40 12.0	6.40 12.0	6.40 12.0
"	6.60 12.0	6.60 12.0	6.60 18.0	6.60 18.0	8.00 26.0	8.00 26.0	8.05 26.0	8.05 26.0	8.15 26.0	8.15 26.0	8.15 26.0	8.15 26.0
"	8.10 26.0	8.10 26.0	8.00 26.0	8.00 26.0								